www.ietdl.org

Published in IET Control Theory and Applications
Received on 1st May 2010
Revised on 5th November 2010
doi: 10.1049/iet-cta.2010.0228

Special Issue on Continuous-time Model Identification

ISSN 1751-8644

Continuous-time predictor-based subspace identification using Laguerre filters

M. Bergamasco M. Lovera

Dipartimento di Elettronica e Informazione, Politecnico di Milano, Piazza Leonardo da Vinci 32, 20133 Milano, Italy
E-mail: lovera@elet.polimi.it

Abstract: This study deals with the problem of continuous-time model identification and presents two subspace-based algorithms capable of dealing with data generated by systems operating in closed loop. The algorithms are developed by reformulating the identification problem from the continuous-time model to equivalent ones to which discrete-time subspace identification techniques can be applied. More precisely, two approaches are considered, the former leading to the so-called all-pass domain by using a bank of Laguerre filters applied to the input–output data and the latter corresponding to the projection of the input–output data onto an orthonormal basis, again defined in terms of Laguerre filters. In both frameworks, the Predictor-Based Subspace Identification, originally developed in the case of discrete-time systems, can be reformulated for the continuous-time case. Simulation results are used to illustrate the achievable performance of the proposed approaches with respect to existing methods available in the literature.

1 Introduction

System identification is today a very mature research area, the results of which find application in a very diverse range of fields. Although most of the literature on system identification focuses on discrete-time models, in many situations of practical interest (e.g. aircraft and rotorcraft identification, see e.g. [1, 2]) the direct estimation of the parameters of a continuous-time model from sampled input–output data is an important problem per se, for which dedicated methods and tools have to be employed. Moreover, the problem of identifying models under special circumstances which turn out to be critical in discrete-time, such as the identification of stiff systems or the use of non-equidistantly sampled data, make it necessary to develop special algorithms that can deal with these cases. The development of identification methods for continuous-time models is a challenge of its own, and has been studied extensively (see e.g. the recent book [3] and the references therein).

In the last 20 years or so, subspace model identification (SMI) algorithms have been developed, which have proven extremely successful in dealing with the estimation of discrete-time state-space models for multiple input–multiple output (MIMO) systems. Not surprisingly, the problem of extending SMI methods to the identification of continuous-time systems has been studied in a number of contributions. In [4] a frequency-domain approach to subspace identification of continuous-time models was proposed, whereas a time-domain SMI algorithm able to identify a continuous-time model from sampled input–output data was first proposed in [5], building on the framework introduced in [6]. More precisely, in the cited thesis the MIMO Output-Error State sPace (MOESP, see [7]) class of SMI algorithms was extended to the identification of continuous-time models through the use of Laguerre filters: this allowed the development of a method that deals with noise in a similar way as its discrete-time counterparts. More recently, in [8] the version of the MOESP algorithm presented in [9, 10] is adopted and a discrete-time algebraic equation is derived starting from sampled input–output data by describing derivatives of stochastic processes in the distribution sense, whereas in [11, 12] the combination of the MOESP algorithm with filtering methods to avoid the need to compute numerical derivatives of input–output signals was proposed. In [13] a novel approach to the problem of continuous-time SMI has been presented, based on the adoption of orthonormal basis functions to arrive, again, at a MOESP-like data equation for a continuous-time system.

All the above-mentioned contributions, however, assume that the system under study is operating in open-loop. This assumption is frequently restrictive in practice and is typically violated, for example, in the above-mentioned aerospace applications, in which partial loop closures must be retained during identification experiments, primarily for safety issues. The problem of closed-loop SMI has been studied extensively in recent years due to its high relevance for practical applications (see e.g. [14–17] and the references therein). The present state-of-the-art is represented by the so-called Predictor-Based Subspace IDentification (PBSID) algorithm (see, again, [16]) which, under suitable assumptions, can provide consistent estimates of the state-space matrices for a discrete-time, linear time-invariant system operating under feedback. To the best knowledge of the authors, the problem of closed-loop subpace identification in continuous-time has been only considered in the literature in [18], where the application of

the errors-in-variables approach of [15] is proposed to deal with correlation in a continuous-time setting.

In the light of the above discussion, the aim of this paper is to propose novel continuous-time SMI schemes, based on the derivation of PBSID-like algorithms within the all-pass domains proposed in [5, 13] and relying, respectively, on Laguerre filtering and Laguerre projections of the sampled input–output data. The performance of the proposed approaches with respect to existing subspace algorithms for the continuous-time problem will be demonstrated in a simulation study.

The paper is organised as follows: Section 2 provides a concise statement of the continuous-time SMI problem, whereas the proposed approaches, together with the relevant background, are presented in detail in Sections 3 and 4. Issues related with the actual discrete-time implementation of the algorithms are highlighted in Section 5, whereas simulation results are presented and discussed in Section 6.

2 Problem statement and preliminaries

Consider the linear, time-invariant continuous-time system

$$\begin{aligned} \mathrm{d}x(t) &= Ax(t)\,\mathrm{d}t + Bu(t)\,\mathrm{d}t + \mathrm{d}w(t), \quad x(0) = x_0 \\ \mathrm{d}z(t) &= Cx(t)\,\mathrm{d}t + Du(t)\,\mathrm{d}t + \mathrm{d}v(t) \\ y(t)\mathrm{d}t &= \mathrm{d}z(t) \end{aligned} \tag{1}$$

where $x \in \mathbb{R}^n$, $u \in \mathbb{R}^m$ and $y \in \mathbb{R}^p$ are, respectively, the state, input and output vectors and $w \in \mathbb{R}^n$ and $v \in \mathbb{R}^n$ are the process and the measurement noise, respectively, modelled as Wiener processes with incremental covariance given by

$$E\left\{\begin{bmatrix} \mathrm{d}w(t) \\ \mathrm{d}v(t) \end{bmatrix}\begin{bmatrix} \mathrm{d}w(t) \\ \mathrm{d}v(t) \end{bmatrix}^{\mathrm{T}}\right\} = \begin{bmatrix} Q & S \\ S^{\mathrm{T}} & R \end{bmatrix}\mathrm{d}t$$

The system matrices A, B, C and D, of appropriate dimensions, are such that (A, C) is observable, $(A, [B, Q^{1/2}])$ is controllable and A is asymptotically stable. Assume that a dataset $\{u(t_i), y(t_i)\}$, $i \in [1, N]$ of sampled input/output data (possibly associated with a non equidistant sequence of sampling instants) obtained from system (1) is available. Then, the problem is to provide a consistent estimate of the state-space matrices A, B, C and D (up to a similarity transformation) on the basis of the available data.

In the following sections, a number of definitions will be used, which are summarised hereafter for the sake of clarity. See, for example, [6, 19, 20] for further details.

Let $\mathcal{L}_2(0, \infty)$ denote the space of square integrable and Lebesgue measurable functions of time $0 < t < \infty$, with the inner product defined as $\langle f, g\rangle = \int_0^\infty f(t)g(t)\,\mathrm{d}t$, for f, $g \in \mathcal{L}_2(0, \infty)$; the space $\mathcal{H}_2$ is the closed subspace of $\mathcal{L}_2(i\mathbb{R})$ with functions analytic in the open right half plane, with norm

$$\|U\|_2^2 = \sup_{\sigma>0}\frac{1}{2\pi}\int_{-\infty}^{\infty}|U(\sigma + j\omega)|^2\,\mathrm{d}\omega = \frac{1}{2\pi}\int_{-\infty}^{\infty}|U(j\omega)|^2\,\mathrm{d}\omega \tag{2}$$

In view of Parseval's relation, the spaces $\mathcal{L}_2(0, \infty)$ and $\mathcal{H}_2$ are related by the isometric isomorphism defined by the bilateral Fourier transform, so if $U \in \mathcal{H}_2$, the inverse Fourier transform $u = \mathcal{F}^{-1}[U]$ is in $\mathcal{L}_2(0, \infty)$ and $\|U\|_2 = \|u\|_2$.

A scalar transfer function $w(s)$ is called inner if it is a bounded analytic function in the open right half plane (i.e. $w(j\omega) \in \mathcal{H}_\infty$), such that $|w(j\omega)| = 1$ or $\tilde{w}(j\omega)w(j\omega) = 1$ almost everywhere on the imaginary axis, where $\tilde{w}(j\omega) = w^{\mathrm{T}}(-j\omega)$ is the para-conjugate (i.e. w is an all-pass transfer function). We further denote by Λ_w the multiplication operator $\mathcal{L}_2(0, \infty) \mapsto \mathcal{L}_2(0, \infty)$ defined as

$$\Lambda_w u(t) = \mathcal{F}^{-1}[w\mathcal{F}[u(t)]] \tag{3}$$

In the following, the focus will be on the first-order inner function

$$w(s) = \frac{s-a}{s+a} \tag{4}$$

$a > 0$, together with the associated realisation

$$w(s) = \frac{c_w b_w}{s - a_w} + d_w \tag{5}$$

where $a_w = -a$, $b_w = -\sqrt{2a}$, $c_w = \sqrt{2a}$, $d_w = 1$. Then, it can be shown that $w(s)\mathcal{H}_2$ is a proper closed subspace of $\mathcal{H}_2$, the orthogonal complement of which is denoted as $S = \mathcal{H}_2 \ominus w(s)\mathcal{H}_2$, that

$$\mathcal{L}_0(s) = \frac{c_w}{s+a} = \frac{\sqrt{2a}}{s+a} \tag{6}$$

is a basis of the (one-dimensional) subspace S and that the set

$$\{\mathcal{L}_0, w\mathcal{L}_0, \ldots, w^i\mathcal{L}_0, \ldots\} \tag{7}$$

is an orthonormal basis of $\mathcal{H}_2$, that is, $\mathcal{H}_2 = \oplus_{i=0}^{\infty} w^i S$. Equivalently, letting $\ell_0 = \mathcal{F}^{-1}[\mathcal{L}_0]$, the set

$$\{\ell_0, \Lambda_w\ell_0, \ldots, \Lambda_w^i\ell_0, \ldots\} \tag{8}$$

is an orthonormal basis of $\mathcal{L}_2(0, \infty)$, that is, $\mathcal{L}_2(0, \infty) = \oplus_{i=0}^{\infty}\Lambda_w^i S$.

The transfer function of the ith (order $i + 1$) Laguerre filter is then defined as

$$\mathcal{L}_i(s) = w^i(s)\mathcal{L}_0(s) = \sqrt{2a}\,\frac{(s-a)^i}{(s+a)^{i+1}} \tag{9}$$

Note that in the following, in accordance with the notation of [5], the Laguerre-like filters

$$L_i(s) = 2a\,\frac{(s-a)^i}{(s+a)^{i+1}} = (1-w)w^i \tag{10}$$

will also be used. In the time domain, we will denote with $w^i(t)$ the impulse response of the concatenation of the first ith order all-pass filters and by $[w^i u](t)$ the convolution of $u(t)$ and $w^i(t)$, that is, $[w^i u](t) = \int_0^t w^i(t-\tau)u(\tau)\,\mathrm{d}\tau$. Similarly, $l_i(t)$ is the impulse response of the ith Laguerre-like filter $L_i(s)$ and $[l_i u](t)$ denotes the convolution of $u(t)$ and $l_i(t)$, that is, $[l_i u](t) = \int_0^t l_i(t-\tau)u(\tau)\,\mathrm{d}\tau$.

The Laguerre basis and its generalisations to wider classes of orthonormal basis functions (see e.g. the classical references ([21–23]) have been used extensively in the system identification literature in order to formulate the system identification problem for continuous-time

input–output models as a linear-in-the-parameters one. In this work, however, the properties of the Laguerre basis will be exploited in a different way, that is, with the goal of converting continuous-time models into equivalent discrete-time ones, as discussed in the following sections.

3 From continuous-time to discrete-time using Laguerre filters

The main issue in the application of SMI methods to continuous-time systems is the need of computing the high-order derivatives of input–output measurements arising from the continuous-time data equation. This problem has been faced in the literature using a number of different approaches, of which two will be considered in the present study.

3.1 First approach: Laguerre filtering

The first approach relies on the idea, first proposed in [6] and further developed in [5], of resorting to the bilinear transformation associated with a first-order all-pass filter in order to convert the derivative operation to *low-pass* filtering based on the class of Laguerre orthogonal filters. It can be shown that an input–output data equation similar to the one for discrete-time state-space models can be derived, to which SMI techniques can be applied.

On the basis of the definitions given in the previous section, according to [5, Lemma 3.4] and considering the Laguerre-like filters defined in (10), the state-space model (1) can be equivalently written as

$$\begin{aligned}[wx](t) &= A_w x(t) + B_w[l_0 u](t) + [l_0 w_w](t) + F_1 x_0 l_0(t)\\ [l_0 y](t) &= C_w x(t) + D_w[l_0 u](t) + [l_0 v_w](t) + F_2 x_0 l_0(t)\end{aligned} \tag{11}$$

where the state-space matrices are given by

$$\begin{aligned}A_w &= (A + aI)^{-1}(A - aI)\\ B_w &= (A + aI)^{-1}B\\ C_w &= 2aC(A + aI)^{-1}\\ D_w &= D - C(A + aI)^{-1}B\\ F_1 &= (A + aI)^{-1}\\ F_2 &= C(A + aI)^{-1}\end{aligned} \tag{12}$$

the new noise processes w_w and v_w are defined as

$$\begin{aligned}w_w(t)\,\mathrm{d}t &= (A + aI)^{-1}\,\mathrm{d}w(t)\\ v_w(t)\,\mathrm{d}t &= \mathrm{d}v(t) - C(A + aI)^{-1}\,\mathrm{d}w(t)\end{aligned} \tag{13}$$

and x_0 is the initial state of the original continuous-time system.

System (11) can be equivalently written in innovation form

$$\begin{aligned}[w\hat{x}](t) &= A_w\hat{x}(t) + B_w[l_0 u](t) + K_w[l_0 e](t) + F_1 x_0 l_0(t)\\ [l_0 y](t) &= C_w\hat{x}(t) + D_w[l_0 u](t) + [l_0 e](t) + F_2 x_0 l_0(t)\end{aligned} \tag{14}$$

where the Kalman gain K_w is related to the Kalman gain K of (1) by

$$\begin{aligned}P_w &= A_w P_w A_w^{\mathrm{T}} + Q_w - (A_w P_w C_w^{\mathrm{T}} + S_w^{\mathrm{T}})\\ &\quad\times (C_w P_w C_w^{\mathrm{T}} + R_w)^{-1}(C_w P_w A_w^{\mathrm{T}} + S_w)\end{aligned}$$

$$K_w = (A_w P_w C_w^{\mathrm{T}} + S_w^{\mathrm{T}})(C_w P_w C_w^{\mathrm{T}} + R_w)^{-1}$$

where

$$E\left\{\begin{bmatrix} w_w(t)\,\mathrm{d}t\\ v_w(t)\,\mathrm{d}t\end{bmatrix}\begin{bmatrix} w_w(t)\,\mathrm{d}t\\ v_w(t)\,\mathrm{d}t\end{bmatrix}^{\mathrm{T}}\right\} = \begin{bmatrix} Q_w & S_w\\ S_w^{\mathrm{T}} & R_w\end{bmatrix}\mathrm{d}t$$

Remark 1: It is interesting to point out that in view of the choice of using stable Laguerre filters to operate on the input–output data, the bilinear transformation relating the continuous-time state-space matrices to the equivalent discrete-time ones is not the classical mapping from the open left half plane to the open unit disk. Indeed, it is easy to see that the transformation relating A_w and A maps eigenvalues of A located in the open left half plane into eigenvalues of A_w located outside the open unit disk.

3.2 Second approach: Laguerre projections

The second approach, based on the results first presented in [13, 20] and summarised in Section 2, allows one to obtain a discrete-time equivalent model starting from the continuous-time system (1), along the following lines. First note that under the assumptions stated in Section 2, (1) can be written in innovation form as

$$\begin{aligned}\mathrm{d}x(t) &= Ax(t)\,\mathrm{d}t + Bu(t)\,\mathrm{d}t + K\mathrm{d}e(t)\\ \mathrm{d}z(t) &= Cx(t)\,\mathrm{d}t + Du(t)\,\mathrm{d}t + \mathrm{d}e(t)\\ y(t)\,\mathrm{d}t &= \mathrm{d}z(t)\end{aligned} \tag{15}$$

and it is possible to apply the results of [13] to derive a discrete-time equivalent model, as follows. Consider the first-order inner function $w(s)$ and apply to the input u, the output y and the innovation e of (15) the transformations

$$\begin{aligned}\tilde{u}(k) &= \int_0^\infty \Lambda_w^k \ell_0(t)u(t)\,\mathrm{d}t\\ \tilde{y}(k) &= \int_0^\infty \Lambda_w^k \ell_0(t)y(t)\,\mathrm{d}t\\ \tilde{e}(k) &= \int_0^\infty \Lambda_w^k \ell_0(t)\mathrm{d}e(t)\end{aligned} \tag{16}$$

where $\tilde{u}(k) \in \mathbb{R}^m$, $\tilde{e}(k) \in \mathbb{R}^p$ and $\tilde{y}(k) \in \mathbb{R}^p$. Then (see [13] for details) the transformed system has the state-space representation as

$$\begin{aligned}\xi(k+1) &= A_o\xi(k) + B_o\tilde{u}(k) + K_o\tilde{e}(k), \quad \xi(0) = 0\\ \tilde{y}(k) &= C_o\xi(k) + D_o\tilde{u}(k) + \tilde{e}(k)\end{aligned} \tag{17}$$

IET Control Theory Appl., 2011, Vol. 5, Iss. 7, pp. 856–867
doi: 10.1049/iet-cta.2010.0228

where the state-space matrices are given by

$$\begin{aligned} A_o &= (A - aI)^{-1}(A + aI) \\ B_o &= \sqrt{2a}(A - aI)^{-1}B \\ C_o &= -\sqrt{2a}C(A - aI)^{-1} \\ D_o &= D - C(A - aI)^{-1}B \end{aligned} \tag{18}$$

Remark 2: As in the case of the Laguerre filtering approach, it is interesting to focus on the bilinear transformation relating the matrix A of the continuous-time system (15) with the corresponding matrix A_o of the discrete-time equivalent. It is apparent that in this case the conventional bilinear transformation (i.e. the one mapping the open left half plane into the open unit disk) is used, so the stability of A is preserved in the process.

4 Continuous-time predictor-based subspace model identification

On the basis of the approaches described in the previous section to the derivation of discrete-time equivalent models for the system (1), in this section two algorithms for continuous-time subspace model identification based on the predictor-based idea first proposed in [16] are presented and discussed.

4.1 Predictor-based identification using Laguerre filtering

Considering system (14) in the all-pass domain, a PBSID-like approach to the estimation of the state-space matrices A_w, B_w, C_w, D_w, K_w, F_1 and F_2 can be derived. To this purpose, note that according to [5, Theorem 3.9], the Kalman filter associated with system (14) in the all-pass domain can be written as

$$\begin{aligned} [w\hat{x}](t) &= \bar{A}_w\hat{x}(t) + \bar{B}_w[l_0u](t) + K_w[l_0y](t) + \bar{F}_wx_0l_0(t) \\ &= \bar{A}_w\hat{x}(t) + \tilde{B}_w[l_0z](t) \end{aligned} \tag{19}$$

where

$$\bar{A}_w = A_w - K_wC_w$$

$$\bar{B}_w = B_w - K_wD_w$$

$$\bar{F}_w = F_1 - K_wF_2$$

$$\tilde{B}_w = \begin{bmatrix} \bar{B}_w & K_w & \bar{F}_wx_0 \end{bmatrix}$$

and

$$[l_0z](t) = \begin{bmatrix} [l_0u](t) \\ [l_0y](t) \\ l_0(t) \end{bmatrix} \tag{20}$$

Iterating $p - 1$ times the filtering operation in the all-pass domain (where p is the so-called past window length) one obtains

$$\begin{aligned} [w^2\hat{x}](t) &= \bar{A}_w^2\hat{x}(t) + \begin{bmatrix} \bar{A}_w\tilde{B}_w & \tilde{B}_w \end{bmatrix}\begin{bmatrix} [l_0z](t) \\ [l_0z](t) \end{bmatrix} \\ &\vdots \\ [w^p\hat{x}](t) &= \bar{A}_w^p\hat{x}(t) + \mathcal{K}^pZ_0^{p-1}(t) \end{aligned} \tag{21}$$

where

$$\mathcal{K}^p = \begin{bmatrix} \bar{A}_w^{p-1}\tilde{B}_w & \dots & \tilde{B}_w \end{bmatrix} \tag{22}$$

is the extended controllability matrix of the system in the all-pass domain and

$$Z_0^{p-1}(t) = \begin{bmatrix} [l_0z](t) \\ \vdots \\ [l_{p-1}z](t) \end{bmatrix}$$

Under the considered assumptions, $\bar{A}_w$ has all the eigenvalues inside the open unit circle, so the term $\bar{A}_w^px(t)$ is negligible for sufficiently large values of p and we have that $[w^p\hat{x}](t) \simeq \mathcal{K}^pZ_0^{p-1}(t)$. As a consequence, denoting with f the future window length, the input–output behaviour of the system is approximately given by

$$\begin{aligned} [l_py](t) &\simeq C_w\mathcal{K}^pZ_0^{p-1}(t) + D_w[l_pu](t) + F_2x_0l_p(t) + [l_pe](t) \\ &\vdots \\ [l_{p+f}y](t) &\simeq C_w\mathcal{K}^pZ_f^{p+f-1}(t) + D_w[l_{p+f}u](t) \\ &\quad + F_2x_0l_{p+f}(t) + [l_{p+f}e](t) \end{aligned} \tag{23}$$

so that introducing the vector notation

$$Y^{p,f}(t) = \begin{bmatrix} [l_py](t) & [l_{p+1}y](t) & \dots & [l_{p+f}y](t) \end{bmatrix}$$

$$U^{p,f}(t) = \begin{bmatrix} [l_pu](t) & [l_{p+1}u](t) & \dots & [l_{p+f}u](t) \end{bmatrix}$$

$$E^{p,f}(t) = \begin{bmatrix} [l_pe](t) & [l_{p+1}e](t) & \dots & [l_{p+f}e](t) \end{bmatrix}$$

$$\Psi^{p,f}(t) = \begin{bmatrix} l_p(t) & l_{p+1}(t) & \dots & l_{p+f}(t) \end{bmatrix}$$

$$X^{p,f}(t) = \begin{bmatrix} [w^px](t) & [w^{p+1}x](t) & \dots & [w^{p+f}x](t) \end{bmatrix}$$

$$\bar{Z}^{p,f}(t) = \begin{bmatrix} Z_0^{p-1}(t) & Z_1^p(t) & \dots & Z_f^{p+f-1}(t) \end{bmatrix}$$

(21) and (23) can be rewritten as

$$\begin{aligned} X^{p,f}(t) &\simeq \mathcal{K}^p\bar{Z}^{p,f}(t) \\ Y^{p,f}(t) &\simeq C_w\mathcal{K}^p\bar{Z}^{p,f}(t) + D_wU^{p,f}(t) + F_2x_0\Psi^{p,f}(t) + E^{p,f}(t) \end{aligned} \tag{24}$$

Considering now the sampled input–output data instead of the continuous-time evolution of the relevant signals, the

data matrices become

$$Y_N^{p,f} = \left[[l_p y](t_1) \ \dots \ [l_p y](t_N) \ \dots \ [l_{p+f} y](t_1) \ \dots \ [l_{p+f} y](t_N) \right] \tag{25}$$

and similarly for $U^{p,f}(t)$, $E^{p,f}(t)$, $\Psi^{p,f}(t)$, $X^{p,f}(t)$ and $\bar{Z}^{p,f}(t)$. The data equations (24), in turn, are given by

$$\begin{aligned} X_N^{p,f} &\simeq \mathcal{K}^p \bar{Z}_N^{p,f} \\ Y_N^{p,f} &\simeq C_w \mathcal{K}^p \bar{Z}_N^{p,f} + D_w U_N^{p,f} + F_2 x_0 \Psi_N^{p,f} + E_N^{p,f} \end{aligned} \tag{26}$$

From this point on, the algorithm can be developed along the lines of the discrete-time PBSID$_{\text{opt}}$ method, that is, by carrying out the following steps in which the past and future window lengths are considered equals (i.e. $f = p$). Estimates of the matrices $C_w \mathcal{K}^p$, D_w and $F_2 x_0$ are first computed by solving the least-squares problem

$$\min_{C_w \mathcal{K}^p, D_w, F_2 x_0} \| Y_N^{p,p} - C_w \mathcal{K}^p \bar{Z}_N^{p,p} - D_w U_N^{p,p} - F_2 x_0 \Psi_N^{p,p} \|_F \tag{27}$$

The estimates of $F_2 x_0$ and of D_w provide information, respectively, on the effect of the initial state of the system on the future outputs and on the direct feedthrough term. The estimate of $C_w \mathcal{K}^p$, on the other hand, is useful in computing an estimate of the state sequence for the system, as described in the following. First note that defining the extended observability matrix Γ^p as

$$\Gamma^p = \begin{bmatrix} C_w \\ C_w \bar{A}_w \\ \vdots \\ C_w \bar{A}_w^{p-1} \end{bmatrix} \tag{28}$$

the product of Γ^p and $\mathcal{K}^p$ can be written as

$$\begin{aligned} \Gamma^p \mathcal{K}^p &= \begin{bmatrix} C_w \bar{A}_w^{p-1} \tilde{B}_w & \dots & C_w \tilde{B}_w \\ C_w \bar{A}_w^{p} \tilde{B}_w & \dots & C_w \bar{A}_w \tilde{B}_w \\ \vdots & & \\ C_w \bar{A}_w^{2p-2} \tilde{B}_w & \dots & C_w \bar{A}_w^{p-1} \tilde{B}_w \end{bmatrix} \\ &\simeq \begin{bmatrix} C_w \bar{A}_w^{p-1} \tilde{B}_w & \dots & C_w \tilde{B}_w \\ 0 & \dots & C_w \bar{A}_w \tilde{B}_w \\ \vdots & & \\ 0 & \dots & C_w \bar{A}_w^{p-1} \tilde{B}_w \end{bmatrix} \end{aligned} \tag{29}$$

where the approximation holds provided that p is sufficiently large to have $\bar{A}_w^k \simeq 0$ for $k \geq p$. In view of the definition of $\mathcal{K}^p$ in (22), one can see that the first block row in the product $\Gamma^p \mathcal{K}^p$ can be computed using the estimate $\widehat{C_w \mathcal{K}^p}$ of $C_w \mathcal{K}^p$ obtained by solving the least-squares problem (27), while the subsequent block rows can be obtained by exploiting the shift structure apparent from the right-hand side of (29).

Recalling now that

$$X_N^{p,p} \simeq \mathcal{K}^p \bar{Z}_N^{p,p} \tag{30}$$

it also holds that

$$\Gamma^p X_N^{p,p} \simeq \Gamma^p \mathcal{K}^p \bar{Z}_N^{p,p} \tag{31}$$

Therefore computing the singular value decomposition

$$\Gamma^p \mathcal{K}^p \bar{Z}_N^{p,p} = U \Sigma V^{\mathrm{T}} \tag{32}$$

an estimate of the state sequence can be obtained as

$$\widehat{X}_N^{p,p} = \Sigma_n V_n^{\mathrm{T}} \tag{33}$$

from which, in turn, an estimate of C_w can be computed by solving the least-squares problem

$$\min_{C_w} \| Y_N^{p,p} - \widehat{D}_w U_N^{p,p} - \widehat{F_2 x_0} \Psi_N^{p,p} - C_w \widehat{X}_N^{p,p} \|_F \tag{34}$$

The final steps consist of the estimation of the innovation data matrix $E_N^{p,p}$

$$E_N^{p,p} = Y_N^{p,p} - \widehat{C}_w \widehat{X}_N^{p,p} - \widehat{D}_w U_N^{p,p} - \widehat{F_2 x_0} \Psi_N^{p,p} \tag{35}$$

and of the entire set of the state-space matrices for the system in the all-pass domain, which can be obtained by solving the least-squares problem

$$\begin{aligned} \min_{A_w, B_w, K_w, F_1 x_0} & \| \widehat{X}_N^{p+1,p} - A_w \widehat{X}_N^{p,p-1} - B_w U_N^{p,p-1} \\ & - K_w E_N^{p,p-1} - F_1 x_0 \Psi_N^{p,p-1} \|_F \end{aligned} \tag{36}$$

Finally, the state-space form for the original continuous-time system can be recovered by means of (12).

4.2 Predictor-based identification using Laguerre projections

Starting from system (15), in this section a sketch of the derivation of a PBSID-like approach to the estimation of the state-space matrices A_o, B_o, C_o, D_o, K_o is presented, the details being consistent with the procedure described in Section 4.1.

Considering the sequence of sampling instants t_i, $i = 1, \dots, N$, the input u, the output y and the innovation e of (15) are subjected to the transformations

$$\begin{aligned} \tilde{u}_i(k) &= \int_0^\infty (\Lambda_w^k \ell_0(\tau)) u(t_i + \tau) \, \mathrm{d}\tau \\ \tilde{e}_i(k) &= \int_0^\infty (\Lambda_w^k \ell_0(\tau)) de(t_i + \tau) \\ \tilde{y}_i(k) &= \int_0^\infty (\Lambda_w^k \ell_0(\tau)) y(t_i + \tau) \, \mathrm{d}\tau \end{aligned} \tag{37}$$

where $\tilde{u}_i(k) \in \mathbb{R}^m$, $\tilde{e}_i(k) \in \mathbb{R}^p$ and $\tilde{y}_i(k) \in \mathbb{R}^p$. Then (see [13] for details) the transformed system has the state-space representation

$$\begin{aligned} \xi_i(k+1) &= A_o \xi_i(k) + B_o \tilde{u}_i(k) + K_o \tilde{e}_i(k), \ \ \xi_i(0) = x(t_i) \\ \tilde{y}_i(k) &= C_o \xi_i(k) + D_o \tilde{u}_i(k) + \tilde{e}_i(k) \end{aligned} \tag{38}$$

where the state-space matrices are given by (18).

doi: 10.1049/iet-cta.2010.0228

Letting now

$$\tilde{z}_i(k) = \begin{bmatrix} \tilde{u}_i^{\mathrm{T}}(k) & \tilde{y}_i^{\mathrm{T}}(k) \end{bmatrix}^{\mathrm{T}}$$

$$\bar{A}_o = A_o - K_o C_o$$

$$\bar{B}_o = B_o - K_o D_o$$

and

$$\tilde{B}_o = \begin{bmatrix} \bar{B}_o & K_o \end{bmatrix}$$

system (38) can be written as

$$\begin{aligned} \xi_i(k+1) &= \bar{A}_o \xi_i(k) + \tilde{B}_o \tilde{z}_i(k), \quad \xi_i(0) = x(t_i) \\ \tilde{y}_i(k) &= C_o \xi_i(k) + D_o \tilde{u}_i(k) + \tilde{e}_i(k) \end{aligned} \tag{39}$$

to which the $\mathrm{PBSID}_{\mathrm{opt}}$ algorithm can be applied, along the lines of the previous subsection, to compute estimates of the state-space matrices A_o, B_o, C_o, D_o, K_o.

5 Implementation issues

For the sake of clarity, in Tables 1 and 2 summaries of the algorithms proposed in Sections 4.1 (denoted in the following as PBSID_w) and 4.2 (denoted in the following as PBSID_o) are provided.

Some additional comments related to the implementation and the choice of the main parameters are in order. First of all, the identification algorithms outlined in the previous section assume that continuous-time filtering of the input–output variables can actually be performed (Section 4.1) or that continuous-time projections of the input–output data on the Laguerre basis can be computed exactly (Section 4.2). This is obviously not the case, so suitable discretisation schemes for the considered Laguerre filters and projection operations must be devised.

Table 1 Summary of the PBSID_w algorithm

Algorithm PBSID_w
1. Compute $[I_i u](t)$, $[I_i y](t)$ for $i = 0, \ldots, p+f$.
2. Build the matrices $Y_N^{p,f}$, $U_N^{p,f}$ and $\bar{Z}_N^{p,f}$ according to (25).
3. Solve the least-squares problem (27) obtaining $C_w\mathcal{K}^p$, D_w, $F_2 x_0$.
4. According to (29) an estimate of $\Gamma^p\mathcal{K}^p$ is obtained using $C_w\mathcal{K}^p$.
5. Compute the SVD of the matrix $\Gamma^p\mathcal{K}^p\bar{Z}_N^{p,f} = U_n\Sigma_n V_n^{\mathrm{T}}$, choose model order by inspecting the singular values.
6. Obtain an estimate of the state sequence using (33).
7. Solve the least-squares problem (34) obtaining C_w.
8. Compute $E_N^{p,f}$ with (35).
9. Solve the least-squares problem (36) obtaining A_w, B_w, K_w and $F_1 x_0$.
10. Use the matrix relations (12) to obtain A, B, C, D, F_1, F_2.

Table 2 Summary of the PBSID_o algorithm

Algorithm PBSID_o
1. Compute $\tilde{u}_i(k)$ and $\tilde{u}_i(k)$ for $k = 0, \ldots, p+f$ and $i = 0, \ldots, N/2$ using (40).
2. Build the matrices $Y_N^{p,f}$, $U_N^{p,f}$ and $\bar{Z}_N^{p,f}$ according to (25).
3. Solve the least-squares problem (27) obtaining $C_o\mathcal{K}^{\mathrm{p}}$ and $\mathrm{D_o}$.
4. According to (29) an estimate of $\Gamma^p\mathcal{K}^p$ is obtained using $C_o\mathcal{K}^p$.
5. Compute the SVD of the matrix $\Gamma^p\mathcal{K}^p\bar{Z}_N^{p,f} = U_n\Sigma_n V_n^{\mathrm{T}}$, choose model order by inspecting the singular values.
6. Obtain an estimate of the state sequence using (33).
7. Solve the least-squares problem (34) obtaining C_o.
8. Compute $E_N^{p,f}$ with (35).
9. Solve the least-squares problem (36) obtaining A_o, B_o and K_o.
10. Use the matrix relations (18) to obtain A, B, C and D.

A detailed analysis of the impact of filter discretisation on the performance of continuous-time SMI algorithms has been carried out in [5]. In particular, it has been shown that a bias term in the estimation of the state-space matrices appears. More precisely, the discrete-time implementation of the filters leads to a perturbation of the estimated column space of the observability matrix of the system, which in turn leads to bias in the estimated state-space matrices. The perturbation is related with the choice of sampling interval (faster sampling implies smaller bias) and with the conditioning of the system under study (the computed upper bound in the perturbation is inversely proportional to the smallest 'system' singular value in the decomposition leading to the estimate of the observability subspace). Similar issues are expected to arise in the operation of the algorithm proposed in Section 4.1; however, a detailed analysis of the effect of filter discretisation on the bias of the computed estimates of the state-space matrices is left as future work. For the purpose of the present study, the Laguerre filters used in the implementation of the algorithm have been implemented in discrete-time by means of a conventional bilinear (Tustin) transformation. Similar comments apply to the data projections on the Laguerre basis (37) adopted in the derivation of the algorithm of Section 4.2, though in the case of the numerical implementation of such operators no detailed study in terms of perturbation analysis is available in the literature. In this work, the approximate implementation

$$\begin{aligned} \tilde{u}_i(k) &= \int_0^{\infty} \Lambda_w^k \ell_0(\tau) u(t_i + \tau)\,\mathrm{d}\tau = \int_{t_i}^{\infty} \Lambda_w^k \ell_0(\tau - t_i) u(\tau)\,\mathrm{d}\tau \\ &\simeq \int_{t_i}^{t_{N/2}+t_i} \Lambda_w^k \ell_0(\tau - t_i) u(\tau)\,\mathrm{d}\tau \end{aligned} \tag{40}$$

and similarly for $\tilde{y}_i(k)$, has been adopted, in which the indefinite integral has to be computed over a sliding window of length equal to half of the duration of the available dataset. Insight into the significance of such effect can be obtained by inspecting the identification results provided in Section 6 for the noise-free case, in which errors are only due to approximations in the discrete-time implementation of the filtering/projection operations.

Finally, concerning the choice of the parameters f and p, the following general comments can be made. The same guidelines as in the case of the discrete-time PBSID algorithm apply. First of all, it is common practice to choose $f = p$, for the sake of simplicity. Then, one has to keep in mind that in view of the need to construct the extended controllability and observability matrices, one has to ensure that $p \geq n$, as a minimum. In addition, p must be sufficiently large to ensure that the term $\bar{A}_w^p x(t)$ is negligible (unfortunately, this can be verified *a posteriori* only). On the other hand, specific constraints on the choice of p arise due to the need of performing the filtering/projection operations

over finite datasets using filters of order up to $2p$. Indeed, it is easy to verify that the impulse responses of the Laguerre-like filters defined in (9) have a settling time which is an increasing function of the filter order k. Since the implementation of both algorithms requires the computation of convolutions/correlations with the impulse response of such filters over time horizons determined by the length of the available dataset, the duration of the experiment provides an upper bound for the maximum value of the settling time of the highest order filter. An approximate value for the settling time of the filter

$$\mathcal{L}_k(s) = \sqrt{2a}\frac{(s-a)^k}{(s+a)^{k+1}}$$

can be written as $(5+2k)/a$, which for $k=2p$ gives $(5+4p)/a$. Therefore denoting with T the duration of the available dataset and letting $\tau = 1/a$, one has the rough guideline $p \leq (aT-5)/4 \simeq 1/4(T/\tau) - 1$ for PBSID$_w$ and $p \leq (aT/2 - 5/4) \simeq 1/8(T/\tau) - 1$ for PBSID$_o$ (the latter in view of the above described implementation (40) for the projection operation).

6 Simulation examples

The performance of the continuous-time SMI algorithms proposed in Sections 4.1 and 4.2 has been evaluated and compared with the one achieved by the continuous-time PO-MOESP algorithms presented, respectively, in [5] (and denoted in the following as PO-MOESP$_w$) and [13] (denoted in the following as PO-MOESP$_o$) in a simulation study in which input–output data have been collected from a stable MIMO system operating first in open loop and then in closed loop.

6.1 Open-loop case

The considered open-loop system is given by the state-space matrices

$$S: \begin{cases} A = \begin{bmatrix} -2 & 1 \\ 0 & -4 \end{bmatrix} & B = \begin{bmatrix} 1 & 0.5 \\ 0 & 1 \end{bmatrix} \\ C = \begin{bmatrix} 1 & 0 \\ 4 & 1 \end{bmatrix} & D = \begin{bmatrix} 0 & 0 \\ 0 & 0 \end{bmatrix} \end{cases} \quad (41)$$

The simulated data have been collected by applying to each input channel of the system a piece-wise constant input with base period $T_p = 0.01$ s, for a duration of 10 s. The input level is chosen randomly according to a Gaussian distribution with zero mean and unit variance. White Gaussian noise of increasing variance has been added to the output in order to assess the influence of decreasing signal-to-noise ratio on the quality of the computed estimates. For the input and output variables the sampling interval $\Delta t = 0.001$ s has been considered. Similar choices for the p and f parameters have been made in the four algorithms, namely $p = f = 10$.

The first issue to be investigated is the role of the choice of the parameter of the Laguerre filter bank a, which is known to be a critical issue for the continuous-time PO-MOESP$_w$ algorithm of [5]. The results obtained repeating the identification exercise for values of a ranging between 10 and 60 with $\sigma_v^2/\sigma_y^2 = 0.01$ are depicted in Fig. 1. As can be seen from the figure, the algorithms provide very different results as a function of a: the bias on the estimates of the eigenvalues increases faster for the PO-MOESP$_o$ algorithm than for the other algorithms but only for very large values of a.

On the other hand, over the, more reasonable, range between 10 and 30, the PBSID$_o$ algorithm leads to a

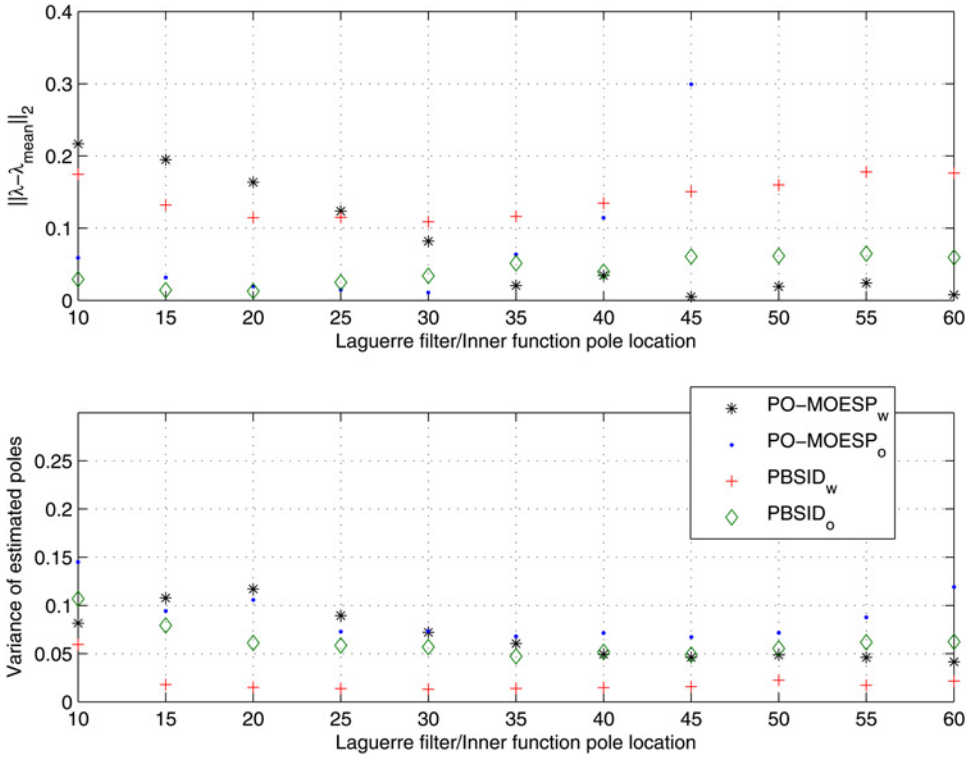

Fig. 1 *Bias and variance of the estimated eigenvalues – open loop experiments*

doi: 10.1049/iet-cta.2010.0228

consistently lower bias and also to a more regular behaviour of the estimation error with respect to the tuning of the Laguerre filters.

Similar comments apply to the variance of the estimated eigenvalues. First of all, the results confirm findings already present in the literature about the somewhat unfavourable behaviour of the estimates of PO-MOESP$_w$ as functions of a. As for the other algorithms, the estimates of the eigenvalues have a similar variance, with PBSID$_w$ consistently providing the best performance.

A more detailed comparison between the performance of the algorithms can be carried out by looking at Tables 3–8,

Table 3 Mean and standard deviation of the eigenvalue estimation error – open-loop experiments with $\Delta t = 0.0005$ s

σ_v^2/σ_y^2	PO-MOESP$_w$	PBSID$_w$
0	0.0000	0.0000
	0.0000	0.0000
0.01	$-0.0759 \pm (0.2462)$	$-0.0612 \pm (0.0899)$
	$0.0059 \pm (0.0185)$	$0.0050 \pm (0.0116)$
0.05	$-0.4981 + 0.0179i \pm (0.5849 + 0.0769i)$	$-0.3159 \pm (0.2039)$
	$0.0605 - 0.0179i \pm (0.0892 + 0.0769i)$	$0.0310 \pm (0.0318)$
0.10	$-0.9837 + 0.1146i \pm (0.7785 + 0.1832i)$	$-0.6727 + 0.0093i \pm (0.3461 + 0.0565i)$
	$0.0633 - 0.1146i \pm (0.2492 + 0.1832i)$	$0.0880 - 0.0093i \pm (0.0927 + 0.0565i)$

Table 4 Mean and standard deviation of the eigenvalue estimation error – open-loop experiments with $\Delta t = 0.0005$ s

σ_v^2/σ_y^2	PO-MOESP$_o$	PBSID$_o$
0	-0.0019	-0.0005
	-0.0000	0.0001
0.01	$-0.0058 \pm (0.2209)$	$0.0065 \pm (0.1819)$
	$0.0018 \pm (0.0180)$	$0.0003 \pm (0.0146)$
0.05	$-0.0338 + 0.0014i \pm (0.6044 + 0.0175i)$	$0.0381 + 0.0007i \pm (0.4383 + 0.0145i)$
	$0.0232 - 0.0014i \pm (0.0726 + 0.0175i)$	$0.0044 - 0.0007i \pm (0.0400 + 0.0145i)$
0.10	$-0.0328 + 0.0104i \pm (0.8385 + 0.0570i)$	$0.0377 + 0.0032i \pm (0.5850 + 0.0345i)$
	$0.0346 - 0.0104i \pm (0.0942 + 0.0570i)$	$0.0066 - 0.0032i \pm (0.0565 + 0.0345i)$

Table 5 Mean and standard deviation of the eigenvalue estimation error – open-loop experiments with $\Delta t = 0.001$ s

σ_v^2/σ_y^2	PO-MOESP$_w$	PBSID$_w$
0	0.0000	0.0000
	0.0000	0.0000
0.01	$-0.1896 + 0.0018i \pm (0.3887 + 0.0249i)$	$-0.1258 \pm (0.1329)$
	$0.0179 - 0.0018i \pm (0.0357 + 0.0249i)$	$0.0097 \pm (0.0176)$
0.05	$-0.9359 + 0.1077i \pm (0.7776 + 0.1783i)$	$-0.6548 + 0.0047i \pm (0.3046 + 0.0355i)$
	$0.0768 - 0.1077i \pm (0.1612 + 0.1783i)$	$0.0857 - 0.0047i \pm (0.0823 + 0.0355i)$
0.10	$-1.6784 + 0.2203i \pm (0.7083 + 0.2226i)$	$-1.3461 + 0.1878i \pm (0.4376 + 0.2210i)$
	$-0.4586 - 0.2203i \pm (1.3915 + 0.2226i)$	$0.2057 - 0.1878i \pm (0.1405 + 0.2210i)$

Table 6 Mean and standard deviation of the eigenvalue estimation error – open-loop experiments with $\Delta t = 0.001$ s

σ_v^2/σ_y^2	PO-MOESP$_o$	PBSID$_o$
0	-0.0066	-0.0016
	-0.0001	0.0002
0.01	$-0.0140 \pm (0.3535)$	$0.0149 \pm (0.2566)$
	$0.0056 \pm (0.0302)$	$0.0012 \pm (0.0214)$
0.05	$-0.0455 + 0.0198i \pm (0.8888 + 0.0846i)$	$0.0314 + 0.0012i \pm (0.6166 + 0.0134i)$
	$0.0377 - 0.0198i \pm (0.0984 + 0.0846i)$	$0.0128 - 0.0012i \pm (0.0639 + 0.0134i)$
0.10	$0.1159 + 0.0560i \pm (1.4410 + 0.1498i)$	$0.0846 + 0.0075i \pm (0.8357 + 0.0506i)$
	$0.0296 - 0.0560i \pm (0.1489 + 0.1498i)$	$0.0174 - 0.0075i \pm (0.0834 + 0.0506i)$

where the results obtained in a Monte Carlo study (averaging over 400 runs, with $a = 20$) are presented. More precisely, the estimation error for the eigenvalues of the system under study has been analysed for decreasing signal-to-noise ratio, as measured on the output. Note that in each table, the first row provides a measure of the estimation error in the noise-free case, which is useful to assess the effect of the implementation aspects discussed in Section 5.

The tables confirm in a more quantitative way the conclusions that were already drawn from the

Table 7 Mean and standard deviation of the eigenvalue estimation error – open-loop experiments with $\Delta t = 0.002$ s

σ_v^2/σ_y^2	PO-MOESP$_w$	PBSID$_w$
0	0.0000	0.0000
	0.0000	0.0000
0.01	$-0.3359 + 0.0058i \pm (0.5329 + 0.0430i)$	$-0.2442 \pm (0.1903)$
	$0.0407 - 0.0058i \pm (0.0719 + 0.0430i)$	$0.0243 \pm (0.0262)$
0.05	$-1.6712 + 0.2163i \pm (0.6731 + 0.2159i)$	$-1.3562 + 0.1799i \pm (0.4193 + 0.2230i)$
	$-0.2785 - 0.2163i \pm (0.9277 + 0.2159i)$	$0.2075 - 0.1799i \pm (0.1434 + 0.2230i)$
0.10	$-2.1092 + 0.1755i \pm (0.3743 + 0.2342i)$	$-2.1122 + 0.4583i \pm (0.3351 + 0.2113i)$
	$-2.0769 - 0.1755i \pm (2.7411 + 0.2342i)$	$-0.2596 - 0.4583i \pm (0.6856 + 0.2113i)$

Table 8 Mean and standard deviation of the eigenvalue estimation error – open-loop experiments with $\Delta t = 0.002$ s

σ_v^2/σ_y^2	PO-MOESP$_o$	PBSID$_o$
0	-0.0119	-0.0024
	0.0012	0.0007
0.01	$-0.0086 + 0.0007i \pm (0.4765 + 0.0142i)$	$0.0572 \pm (0.4104)$
	$0.0123 - 0.0007i \pm (0.0458 + 0.0142i)$	$0.0029 \pm (0.0326)$
0.05	$0.0211 + 0.0575i \pm (1.3199 + 0.1430i)$	$0.0326 + 0.0086i \pm (0.8222 + 0.0510i)$
	$0.0415 - 0.0575i \pm (0.1636 + 0.1430i)$	$0.0207 - 0.0086i \pm (0.0935 + 0.0510i)$
0.10	$0.9662 + 0.0657i \pm (2.9287 + 0.1699i)$	$0.1998 + 0.0276i \pm (1.2204 + 0.1029i)$
	$-0.0226 - 0.0657i \pm (0.2266 + 0.1699i)$	$0.0261 - 0.0276i \pm (0.1307 + 0.1029i)$

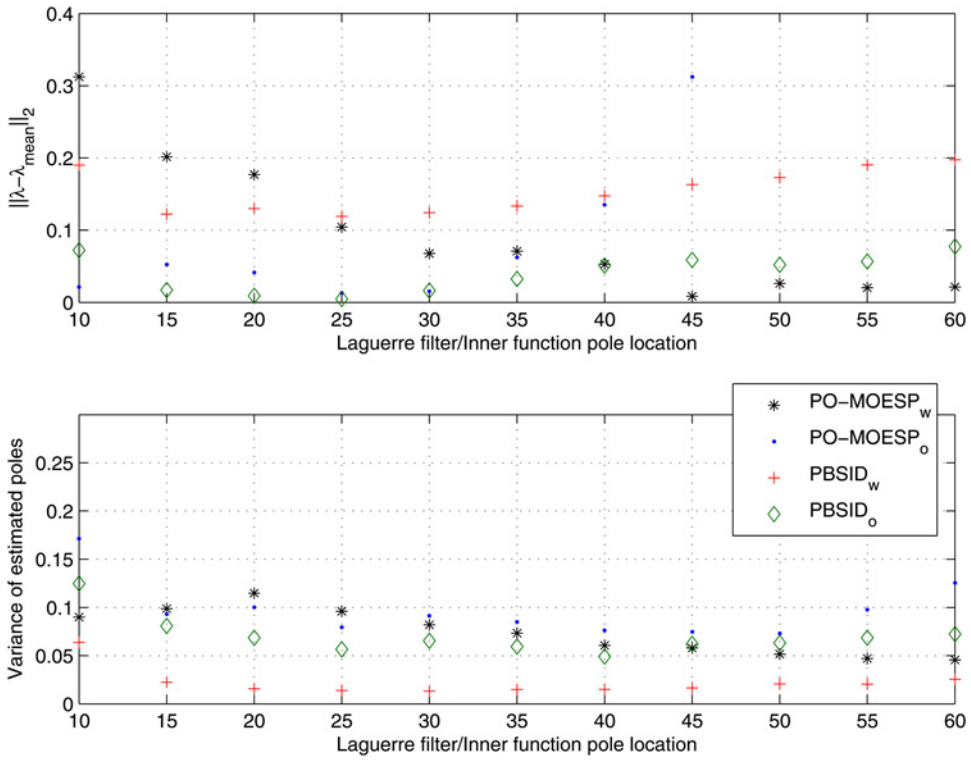

Fig. 2 *Bias and variance of the estimated eigenvalues – closed loop experiments*

doi: 10.1049/iet-cta.2010.0228

Table 9 Mean and standard deviation of the eigenvalue estimation error – closed-loop experiments with $\Delta t = 0.0005$ s

σ_v^2/σ_y^2	PO-MOESP$_w$	PBSID$_w$
0	0.0001	0.0000
	−0.0001	−0.0001
0.01	$-0.0796 \pm (0.2247)$	$-0.0635 \pm (0.0891)$
	$0.0071 \pm (0.0176)$	$0.0053 \pm (0.0113)$
0.05	$-0.3971 + 0.0118i \pm (0.5490 + 0.0603i)$	$-0.2933 \pm (0.1908)$
	$0.0424 - 0.0118i \pm (0.0735 + 0.0603i)$	$0.0275 \pm (0.0289)$
0.10	$-0.8562 + 0.0781i \pm (0.7617 + 0.1527i)$	$-0.5754 + 0.0009i \pm (0.2833 + 0.0175i)$
	$0.0791 - 0.0781i \pm (0.1647 + 0.1527i)$	$0.0701 - 0.0009i \pm (0.0672 + 0.0175i)$

Table 10 Mean and standard deviation of the eigenvalue estimation error – closed-loop experiments with $\Delta t = 0.0005$ s

σ_v^2/σ_y^2	PO-MOESP$_o$	PBSID$_o$
0	−0.0018	−0.0005
	−0.0002	−0.0001
0.01	$-0.0112 \pm (0.2279)$	$0.0090 \pm (0.1791)$
	$0.0038 \pm (0.0193)$	$0.0015 \pm (0.0161)$
0.05	$0.0191 + 0.0028i \pm (0.5548 + 0.0283i)$	$0.0349 \pm (0.3914)$
	$0.0134 - 0.0028i \pm (0.0631 + 0.0283i)$	$0.0042 \pm (0.0352)$
0.10	$-0.0137 + 0.0157i \pm (0.7780 + 0.0782i)$	$0.0799 + 0.0018i \pm (0.5580 + 0.0291i)$
	$0.0274 - 0.0157i \pm (0.0872 + 0.0782i)$	$0.0070 - 0.0018i \pm (0.0544 + 0.0291i)$

Table 11 Mean and standard deviation of the eigenvalue estimation error – closed-loop experiments with $\Delta t = 0.001$ s

σ_v^2/σ_y^2	PO-MOESP$_w$	PBSID$_w$
0	0.0001	0.0001
	−0.0002	−0.0002
0.01	$-0.1472 + 0.0007i \pm (0.3484 + 0.0133i)$	$-0.1057 \pm (0.1241)$
	$0.0135 - 0.0007i \pm (0.0321 + 0.0133i)$	$0.0087 \pm (0.0165)$
0.05	$-0.9007 + 0.0827i \pm (0.7185 + 0.1572i)$	$-0.6012 + 0.0050i \pm (0.3128 + 0.0461i)$
	$0.0816 - 0.0827i \pm (0.1555 + 0.1572i)$	$0.0710 - 0.0050i \pm (0.0694 + 0.0461i)$
0.10	$-1.6069 + 0.2191i \pm (0.7358 + 0.2218i)$	$-1.2672 + 0.1508i \pm (0.4548 + 0.2109i)$
	$-0.2913 - 0.2191i \pm (1.0228 + 0.2218i)$	$0.1889 - 0.1508i \pm (0.1408 + 0.2109i)$

Table 12 Mean and standard deviation of the eigenvalue estimation error – closed-loop experiments with $\Delta t = 0.001$ s

σ_v^2/σ_y^2	PO-MOESP$_o$	PBSID$_o$
0	−0.0062	−0.0018
	−0.0003	0.0000
0.01	$-0.0013 \pm (0.3115)$	$0.0079 \pm (0.2705)$
	$0.0034 \pm (0.0252)$	$0.0002 \pm (0.0218)$
0.05	$-0.0750 + 0.0167i \pm (0.8044 + 0.0745i)$	$0.0267 + 0.0017i \pm (0.5601 + 0.0246i)$
	$0.0315 - 0.0167i \pm (0.0940 + 0.0745i)$	$0.0099 - 0.0017i \pm (0.0639 + 0.0246i)$
0.10	$0.2085 + 0.0411i \pm (1.3649 + 0.1222i)$	$0.0766 + 0.0101i \pm (0.7942 + 0.0606i)$
	$0.0248 - 0.0411i \pm (0.1254 + 0.1222i)$	$0.0138 - 0.0101i \pm (0.0912 + 0.0606i)$

analysis of Fig. 1. Note, in passing, that for low signal-to-noise ratio the continuous-time PO-MOESP$_w$ algorithm leads more frequently to complex estimates of the real eigenvalues.

6.2 Closed-loop case

The second considered example consists in the analysis of data generated by system (41) operating under feedback

Table 13 Mean and standard deviation of the eigenvalue estimation error – closed-loop experiments with $\Delta t = 0.002$ s

σ_v^2/σ_y^2	PO-MOESP$_w$	PBSID$_w$
0	0.0003	0.0002
	−0.0005	−0.0003
0.01	$-0.3457 + 0.0087i \pm (0.4916 + 0.0496i)$	$-0.2265 \pm (0.1612)$
	$0.0380 - 0.0087i \pm (0.0664 + 0.0496i)$	$0.0204 \pm (0.0260)$
0.05	$-1.6185 + 0.1981i \pm (0.7177 + 0.2113i)$	$-1.2375 + 0.1240i \pm (0.4370 + 0.1899i)$
	$-0.2741 - 0.1981i \pm (1.1432 + 0.2113i)$	$0.1953 - 0.1240i \pm (0.1389 + 0.1899i)$
0.10	$-2.0809 + 0.1634i \pm (0.4274 + 0.2218i)$	$-1.9974 + 0.4477i \pm (0.3425 + 0.2100i)$
	$-1.9502 - 0.1634i \pm (2.8723 + 0.2218i)$	$-0.1111 - 0.4477i \pm (0.5686 + 0.2100i)$

Table 14 Mean and standard deviation of the eigenvalue estimation error – closed-loop experiments with $\Delta t = 0.002$ s

σ_v^2/σ_y^2	PO-MOESP$_o$	PBSID$_o$
0	−0.0119	−0.0017
	0.0008	0.0002
0.01	$-0.0105 \pm (0.4562)$	$0.0440 \pm (0.3471)$
	$0.0098 \pm (0.0444)$	$0.0017 \pm (0.0312)$
0.05	$0.0631 + 0.0501i \pm (1.3576 + 0.1340i)$	$0.1111 + 0.0064i \pm (0.8161 + 0.0453i)$
	$0.0282 - 0.0501i \pm (0.1568 + 0.1340i)$	$0.0100 - 0.0064i \pm (0.0872 + 0.0453i)$
0.10	$0.8267 + 0.0697i \pm (2.7292 + 0.1609i)$	$0.1706 + 0.0194i \pm (1.1706 + 0.0901i)$
	$-0.0509 - 0.0697i \pm (0.2717 + 0.1609i)$	$0.0125 - 0.0194i \pm (0.1273 + 0.0901i)$

with the controller

$$R: \begin{cases} A = \begin{bmatrix} -20 & 0 \\ 0 & -30 \end{bmatrix} & B = \begin{bmatrix} 1 & 0 \\ 0 & 1 \end{bmatrix} \\ C = \begin{bmatrix} 1 & 0 \\ 0 & 1 \end{bmatrix} & D = \begin{bmatrix} 0 & 0 \\ 0 & 0 \end{bmatrix} \end{cases} \quad (42)$$

which in turn operates on the basis of noisy measurements of the output. The identification experiments have been carried out using the same input sequence as in the open-loop case, again adding white Gaussian noise of increasing variance to the output to achieve the desired signal-to-noise ratio in closed loop. The results obtained in this second example are summarised in Fig. 2 and in Tables 9–14.

As can be seen from the results, both algorithms provide a very satisfactory performance in terms of eigenvalue estimation accuracy, with PBSID$_o$ leading to smaller variance of the estimated eigenvalues over a wide range of values for the Laguerre parameter a.

7 Concluding remarks

In this paper, the problem of continuous-time model identification has been studied and two subspace-based algorithms have been proposed. The algorithms are based on the reformulation of the identification problem from continuous-time to discrete-time by using either Laguerre filtering of the input–output data or projections of the same data onto the Laguerre basis for the appropriate signal space. In this framework, it has been shown along both lines that the PBSID$_{\text{opt}}$ subspace identification algorithm, originally developed in the case of discrete-time systems, can be reformulated for the continuous-time case. Future work will aim at a more detailed analysis of the effect of digital implementation of the algorithms on the accuracy of the estimates.

8 References

1 Klein, V., Morelli, E.A.: 'Aircraft system identification: theory and practice' (AIAA, 2006)
2 Tischler, M., Remple, R.: 'Aircraft and rotorcraft system identification: engineering methods with flight-test examples' (AIAA, 2006)
3 Garnier, H., Wang, L. (Eds.): 'Identification of continuous-time models from sampled data' (Springer, 2008)
4 Van Overschee, P., De Moor, B.: 'Continuous-time frequency domain subspace system identification', *Signal Process.*, 1996, **52**, (2), pp. 179–194
5 Haverkamp, B.R.J.: 'State space identification: theory and practice'. PhD thesis, Delft University of Technology, 2001
6 Johansson, R., Verhaegen, M., Chou, C.T.: 'Stochastic theory of continuous-time state-space identification', *IEEE Trans. Signal Process.*, 1999, **47**, (1), pp. 41–51
7 Verhaegen, M.: 'Identification of the deterministic part of MIMO state space models given in innovations form from input-output data', *Automatica*, 1994, **30**, (1), pp. 61–74
8 Ohsumi, A., Kameyama, K., Yamagushi, K.I.: 'Subspace identification for continuous-time stochastic systems via distribution-based approach', *Automatica*, 2002, **38**, (1), pp. 63–79
9 Verhaegen, M., Dewilde, P.: 'Subspace model identification, part 1: output error state space model identification class of algorithms', *Int. J. Control*, 1992, **56**, (5), pp. 1187–1210
10 Verhaegen, M., Dewilde, P.: 'Subspace model identification, part 2: analysis of the elementary output error state space model identification algorithm', *Int. J. Control*, 1992, **56**, (5), pp. 1211–1241
11 Bastogne, T., Garnier, H., Sibille, P.: 'A PMF-based subspace method for continuous-time model identification. Application to a multivariable winding process', *Int. J. Control*, 2001, **74**, (2), pp. 118–132
12 Mercère, G., Ouvrard, R., Gilson, M., Garnier, H.: 'Identification de systèmes multivariables à temps continu par approche des sous-espaces', *J. Eur. Syst. Automat.*, 2008, **42**, (2–3), pp. 261–285
13 Ohta, Y., Kawai, T.: 'Continuous-time subspace system identification using generalized orthonormal basis functions'. 16th Int. Symp. Mathematical Theory of Networks and Systems, Leuven, Belgium, 2004

doi: 10.1049/iet-cta.2010.0228

14 Ljung, L., McKelvey, T.: 'Subspace identification from closed loop data', *Signal Process.*, 1996, **52**, (2), pp. 209–215
15 Chou, C.T., Verhaegen, M.: 'Subspace algorithms for the identification of multivariable dynamic error-in-variables state space models', *Automatica*, 1997, **33**, (10), pp. 1857–1869
16 Chiuso, A., Picci, G.: 'Consistency analysis of certain closed-loop subspace identification methods', *Automatica*, 2005, **41**, (3), pp. 377–391
17 Huang, B., Ding, S.X., Qin, S.J.: 'Closed-loop subspace identification: an orthogonal projection approach', *J. Process Control*, 2005, **15**, (1), pp. 53–66
18 Mohd-Moktar, R., Wang, L.: 'Continuous-time state space model identification using closed-loop data'. Second Asia Int. Conf. Modelling & Simulation, Kuala Lumpur, Malaysia, 2008
19 Zhou, K., Doyle, J., Glover, K.: 'Robust and optimal control' (Prentice-Hall, 1996)
20 Ohta, Y.: 'Realization of input-output maps using generalized orthonormal basis functions', *Systems Control Lett.*, 2005, **22**, (6), pp. 437–444
21 Wahlberg, B.: 'System identification using Laguerre models', *IEEE Trans. Autom. Control*, 1991, **36**, (5), pp. 551–562
22 Heuberger, P.S.C., Van den Hof, P.M.J., Bosgra, O.H.: 'A generalized orthonormal basis for linear dynamical systems', *IEEE Trans. Autom. Control*, 2005, **40**, (5), pp. 451–465
23 Wahlberg, B., Mäkilä, P.: 'On approximation of stable linear dynamical systems using Laguerre and Kautz functions', *Automatica*, 1996, **32**, (5), pp. 693–708